JOURNAL OF GEOPHYSICAL RESEARCH, VOL. 106, NO. A7, PAGES 13,105–13,118, JULY 1, 2001

Two distinct substorm onsets

V. M. Mishin,[1] T. Saifudinova,[1] A. Bazarzhapov,[1] C. T. Russell,[2] W. Baumjohann,[3,4] R. Nakamura[3,4] and M. Kubyshkina[5]

Abstract. At times, substorms occur in a particular sequence, where a clear growth phase is followed by a first onset at lower latitudes and a second one involving all latitudes between 60° and 70°. The second onset is followed by a clear recovery phase. In the present paper we present nine such sequences in the form of a superposed epoch analysis. Comparison with solar wind data shows that the second onset occurs when the interplanetary magnetic field turns northward. Determination of the change in the open polar cap magnetic flux using the magnetogram inversion technique method indicates that the first onset occurs during an interval of continuous loading of the tail with new open flux merged at the dayside. Hence, despite showing clear ionospheric signatures of substorm expansion, this onset likely involves the reconnection of closed plasma sheet field lines only, while during the second onset and expansion phase, reconnection clearly proceeds from closed plasma sheet to open lobe field lines.

1. Introduction

The central process of the active phase in the near-Earth neutral line (NENL) model of substorms is reconnection of the open magnetic flux Ψ and, as a result, tail collapse with severance of a large-scale plasmoid [*Russell and McPherron*, 1973; *Hones*, 1979; *Baker et al.*, 1996]. *Baker et al.* [1999] recently concluded, on the basis of observational and numerical modeling data, that the global substorm problem has now largely been solved in favor of the NENL model: the loaded magnetosphere rapidly progresses to the same reconnection configuration irrespective of the detailed localized initiation mechanism. This conclusion is supported with Geotail data by *Nagai et al.* [1998], who utilized positive bay signatures at Kakioka, with amplitudes greater than 10 nT, as the indicator of substorm onsets. Other methods may give another result [e.g., *Liou et al.*, 1999]. It has not been shown yet that all types of ground substorm onsets, including most initial multiple onsets and those onsets, discussed below, with sources in the innermost plasma sheet, are associated with signatures of NENL formation in the midtail.

Alternative models have suggested diverse mechanisms for the principal cause of substorms including current disruption (CD) with a "cross-tail current partial disruption" [*Rothwell et al.*, 1988; *Lui*, 1996; *Lui et al.* 1998; *Kan*, 1998; *Erickson et al.*, 1996; *Maynard et al.*, 1996]. CD models do not presuppose NENL formation as necessary for a typical substorm, although it is not excluded as the result of the CD. The two approaches (CD and NENL) also differ in the physics of the local plasma instabilities that are responsible for the active phase onset. The NENL model assumes the tearing mode, with pinching but without tail current disruption [*Zelenyi et al.*, 1998]. Alternative models assume current-driven instabilities accompanied by a partial current disruption in the near tail, without the open flux reconnection [*Lui*, 1996]. The two models also differ in the region of the tail where the instabilities develop: current disruption (CD) and open tail reconnection (NENL) develop in the near and middle tail, that is, in $|X| \leq 10\ R_E$ and $|X| \geq 20\ R_E$, respectively. It is possible that both processes operate [*Vasyliunas*, 1998] producing different types of substorm onsets in two different latitudinal zones corresponding to sources in the near and midtail, and some supporting results have been published.

Based on data for individual events, *Mishin* [1991] and *Mishin et al.* [1997] have suggested that a typical substorm contains two successive active phases, respectively, without and with clear signatures of predominant reconnection of open magnetic flux in the tail lobes. The first active phase (with initial onsets) is mainly driven. It is observed when the amount of open magnetic flux in the tail is still growing, the total substorm power Q_T is less than Poynting flux ε' from the solar wind in the magnetosphere, and the longitudinal size of the current wedge is small. In the second active phase (with the main expansion onset), unloading predominates. This phase is associated with a deep decrease in the open flux; Q_T becomes more than ε', so that the intramagnetospheric energy source predominates; the longitudinal size of the current wedge is doubled. The initial and total expansion onsets may be separated in time by 30 min and more.

Other supporting evidence for multiple distinct substorm onsets has been presented by several authors. Perhaps the first such report was by *Rostoker* [1968, p4217], who showed that "geomagnetic bay disturbances occur in two stages," the first of which he called the trigger bay and like our onsets were separated by 10 to 30 min. More recently, *Taylor et al.* [1996] and *Maynard et al.* [1997] have inferred that open flux typically did not start to decrease until 20 to 40 min after initial substorm onset. *Fox et al.* [1999] have reported substorm intervals in which a substorm onset involving open flux reconnection follows an onset with only closed flux reconnection with a 25 min delay. *Baker et al.* [1993,

[1]Institute of Solar-Terrestrial Physics, Russian Academy of Sciences, Irkutsk, Russia.
[2]Institute of Geophysics and Planetary Physics, University of California, Los Angeles, California.
[3]Max Planck Institut für Extraterrestrische Physik, Garching, Germany.
[4]Now at Space Research Institute, Austrian Academy of Sciences, Graz, Austria.
[5]Institute of Physics, St. Petersburg State University, St. Petersburg, Russia.

Paper number 2000JA900152.
0148-0227/01/2000JA900152$09.00

1996] and *Pulkkinen et al.* [1998a, 1998b] also described two types of ground substorm onsets that map into the inner and midtail, respectively, being separated in time by 20 to 40 min. The first type is more spatially localized than the second one and is observed during open flux growth. The second type is associated with an open flux decrease. Nevertheless, in the interpretation of the authors, both types of onsets are initiated by NENL formation in the midtail.

Thus the hypothesis that two distinct types of substorm onsets may be successively observed during a typical substorm in two different latitudinal zones corresponding to sources in the near and midtail has extensive observational and theoretical support, but it also meets some opposition. This hypothesis can be tested directly with data from ground-based magnetometers located in two regions whose projections are in the inner and midtail, respectively. This direct test is the main motivation for this paper. As has been mentioned, some supporting results have been published earlier based on data for individual substorms. This paper describes a typical (statistical average) rather than an individual substorm. We perform a superposed analysis using nine substorm events. Additional information used is obtained by utilizing the magnetogram inversion technique (MIT2) [*Mishin*, 1991; *Mishin et al.*, 2000]. In particular, MIT2 makes it possible to study the dynamics (in the course of substorms) of the open magnetic flux Ψ and parameters inferred on the basis of Ψ including ε', total substorm power, QT, and other parameters (see section 4). In the scenario that we suggest, not only do the two types of substorm onsets coexist, but they evolve in succession, being linked by the process of tail stretching and collapse, and they constitute a global instability.

2. Database

Magnetograms of the two types of substorm onsets and their MIT2-parameters were obtained with ground-based magnetometers at geomagnetic latitudes higher than 40^0 (see Figure 1) for the nine substorms listed in Table 1. The solar wind and interplanetary magnetic field (IMF) data for seven of these events were available from ISEE 3 and IMP 8. Two of nine events, without solar wind parameters, are marked by asterisks in Table 1 (events 5 and 6 on May 3, 1986). The listed parameters were obtained for each event under consideration and then averaged by the method of superposed epochs. Separate averages were created for all nine events and for the seven with solar wind data. Superposed tracks of solar wind parameters, *AE*, and corrected *Dst* indices are shown in Figure 2. Error bars are calculated at key times throughout the events to show the statistical accuracy of the data.

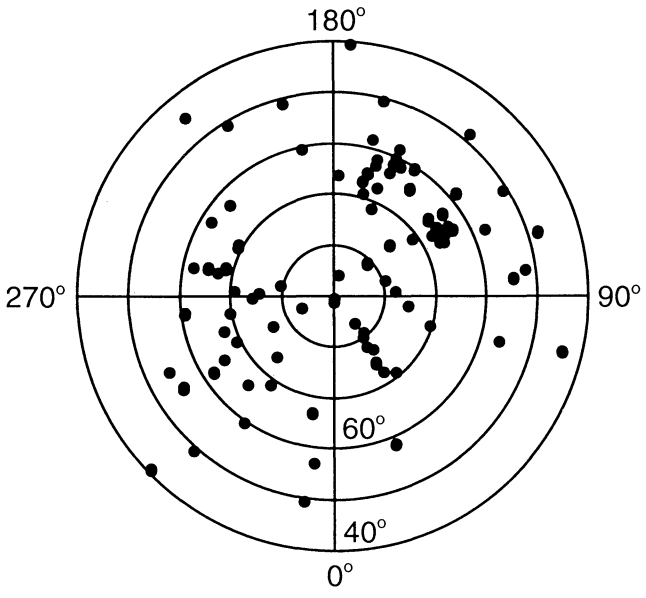

Figure 1. Map of ground-based magnetometers used.

Table 1. Intervals Studied

	Data	Time UT
1	March 22, 1979	1012-1242
2	March 22, 1979	1242-1500
3	April 1, 1986	1810-2200
4	April 2-3, 1986	2150-0500
5[a]	May 3,1986	0050-0155
6[a]	May 3,1986	0900-1030
7	May 8,1986	1100-1500
8	July 24, 1986	2150-2400
9	Dec. 8, 1990	1315-1620

[a] Solar wind data unavailable.

A few of the individual substorms listed in Table 1 have been studied earlier and described in great detail, in particular, the substorms on March 22, 1979 (Coordinated Data Analysis Workshop, CDAW6) [*McPherron and Manka*, 1985, and references therein], May 3, 1986 (CDAW9C) [*Baker et al.*, 1993, and references therein], and July 24, 1986 [*Lui et al.*, 1995]. Some of these independently obtained earlier results will be used in the present paper in comparison with the statistical substorm.

3. Magnetograms of Two Basic Types of Substorm Onsets

A few examples of *X* component magnetograms for the substorms of Table 1 are shown in Figure 3, based on data from different meridional chains of ground-based magnetometers with geomagnetic latitudes greater than 40°. Each chain recorded substorm onsets of one of the events when located in the 21-01 magnetic local time (MLT) sector.

We selected in each magnetogram the first and last onsets marked in Figure 3 by one and two asterisks, respectively. The start time of each last onset was taken to be t=0. After that we selected the greatest first and the greatest last onsets. The stations examined were in the midnight sector, but the station defining onset was not always the one closest to midnight. Thus two groups of magnetograms, each for nine substorms, have been obtained, one for the greatest first and the other for the greatest last onsets. For example, in the March 22, 1979 substorm shown in Figures 3a and 3b, the initial onset at 1054 UT was chosen at the sharp change in slope at the station Meanook. The earlier variation that has no sharp onset is assumed to be part of the growth phase pattern. The main expansion at 1124 UT can be identified best in the Arctic Village record.

The following filter was used in the next step. According to the criterion applied, the interval t<0 should contain the substorm growth phase without onsets and the first active phase which contains all onsets excluding the last one (the number of "first" onsets during one substorm may be greater than unity). The interval $t\geq 0$ should contain the last onset and the recovery. Then, because the duration of each interval, t>0 or t<0, differs from event to event, a normalization was used to match each of the individual substorm phases to an average duration over all selected events, that is, to the duration of the corresponding phase of the average substorm. Two groups of the magnetograms selected and normalized in such a way are shown in Figures 4a and 4b.

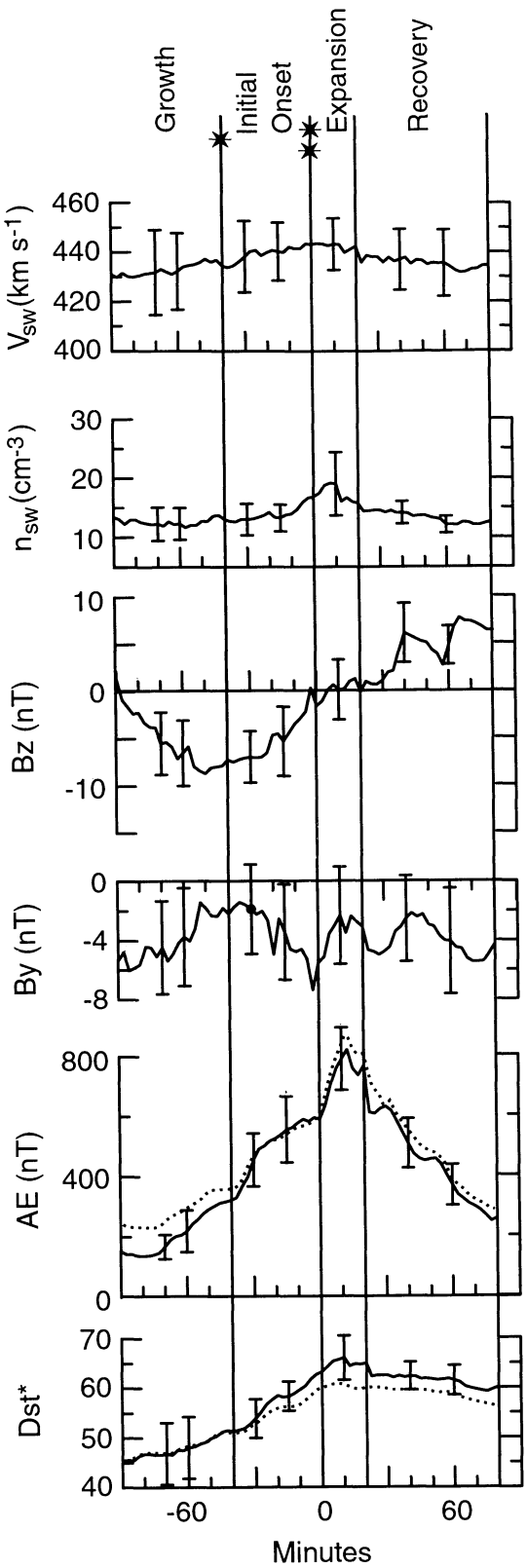

Figure 2. Superposed epoch traces of *AE* and *Dst* indices and solar wind parameters. Solid and dashed lines correspond to superposition of events 7 and 9, respectively (see text).

After such selection and normalization, the selected magnetograms were averaged within each group. For results of this method of superposed epochs see Figures 4c and 4d. The vertical lines in this figure mark both the first onset and the last onset. Figures 4c and 4d show two consecutive and distinct types of onsets in the statistical substorm sequence. The first type (the first onset in the averaged data) is observed in the region 55.2 $<\Phi_1<69.9^0$, with an average latitude $<\Phi_1>=63.4°$, and with an error bar $\Delta\Phi_1=\pm2.5^0$. The onset and expansion of the second type is observed in the same region, but its maximum range was recorded in the region 64.4 $<\Phi_2<$ 72.2^0, that is, in a region with a higher average latitude $<\Phi_2>=68.3\pm2.1^0$. The sign of difference Φ_1-Φ_2 was positive in all events considered. The corresponding values of the neutral sheet geocentric distance $|x|$ have been calculated using the *Tsyganenko* [1989] model for *Kp*=2 and 4, and values of the dipole tilt equal to 2° and -15°. It was found that $|x|$ is larger than 30 R_E and less than 10 R_E, respectively, for Φ=68 and 63°, in all four above-mentioned cases. Note also that Figures 4c and 4d allow us to distinguish four phases in the average substorm sequence: (1) the growth phase without onsets, (2) the first active phase with the first onsets, (3) the second active phase with the last onset, and (4) the recovery phase.

Latitudes, which are characteristic for the first type onset (Φ_1), and the second type (Φ_2), both are dependent on the particular solar wind and magnetospheric conditions. However, the sign of the difference, Φ_2-Φ_1, is always positive to our knowledge, and the basic properties of two types always differ very much, as is shown in Figure 9 for $t<0$ (the first type) and $t>0$ (the second type). Since the error bars on Figure 9 are large, we note that in each of nine studied substorms the plot of each parameter was similar to the relevant superposed plot in Figure 9 [e.g., *Mishin*, 1991; *Mishin et al.*, 1997, 2000, and references therein; *Pulkkinen et al.*, 1998a].

4. Two Types of Substorm Onsets in Terms of Solar Wind and MIT2 Parameters

MIT2 parameters are introduced in this section to be used like solar wind parameters, as characteristic quantities providing the possibility of distinguishing different types of onsets and phases of the average substorm sequence. The magnetogram inversion technique MIT2 is the analogue of the familiar assimilated mapping of ionospheric electrodynamics (AMIE) method [*Kamide et al.*, 1981], which allows the instantaneous spatial distribution to be calculated in latitude-MLT coordinates of the ionospheric electric field and currents, including field-aligned currents (FAC). A detailed description of MIT2 was given recently by *Mishin et al.* [2000]. The polar cap boundary can be determined using the MIT2 spatial distribution of the FAC density as the high-latitude border of FAC Region 1 by *Iijima and Potemra* [1976] or from MIT2 data of the ionospheric electric field as the boundary of the convection reversal. Both methods give results similar within 1°-3° of latitude as needed in this study. MIT2 gives values of the polar cap area *S* compatible with those from other independent methods. By denoting *B* (the average value of geomagnetic field strength in the polar cap ionosphere), one can determine the open magnetic flux through the polar cap as Ψ=*BS*. Figures 5a and 5b allow us to compare Ψ values obtained by MIT2 and the other two methods. It is seen that MIT2 values of Ψ coincide with those from direct methods within 10-20%. A few other tests of the MIT2 method of determining Ψ have been performed by *Mishin et al.* [1992] with similar results.

The open flux Ψ can be represented as the sum $\Psi=\Psi_1+\Psi_2$, where Ψ_2 is the quasipermanent part of Ψ, determined by MIT2 data for quiet conditions before the substorm, and Ψ_1 is a variable part created by recent dayside magnetopause merging. We assume in this paper that Ψ_2 is constant during each substorm under consideration. Only Ψ_1 values will be used in this paper.

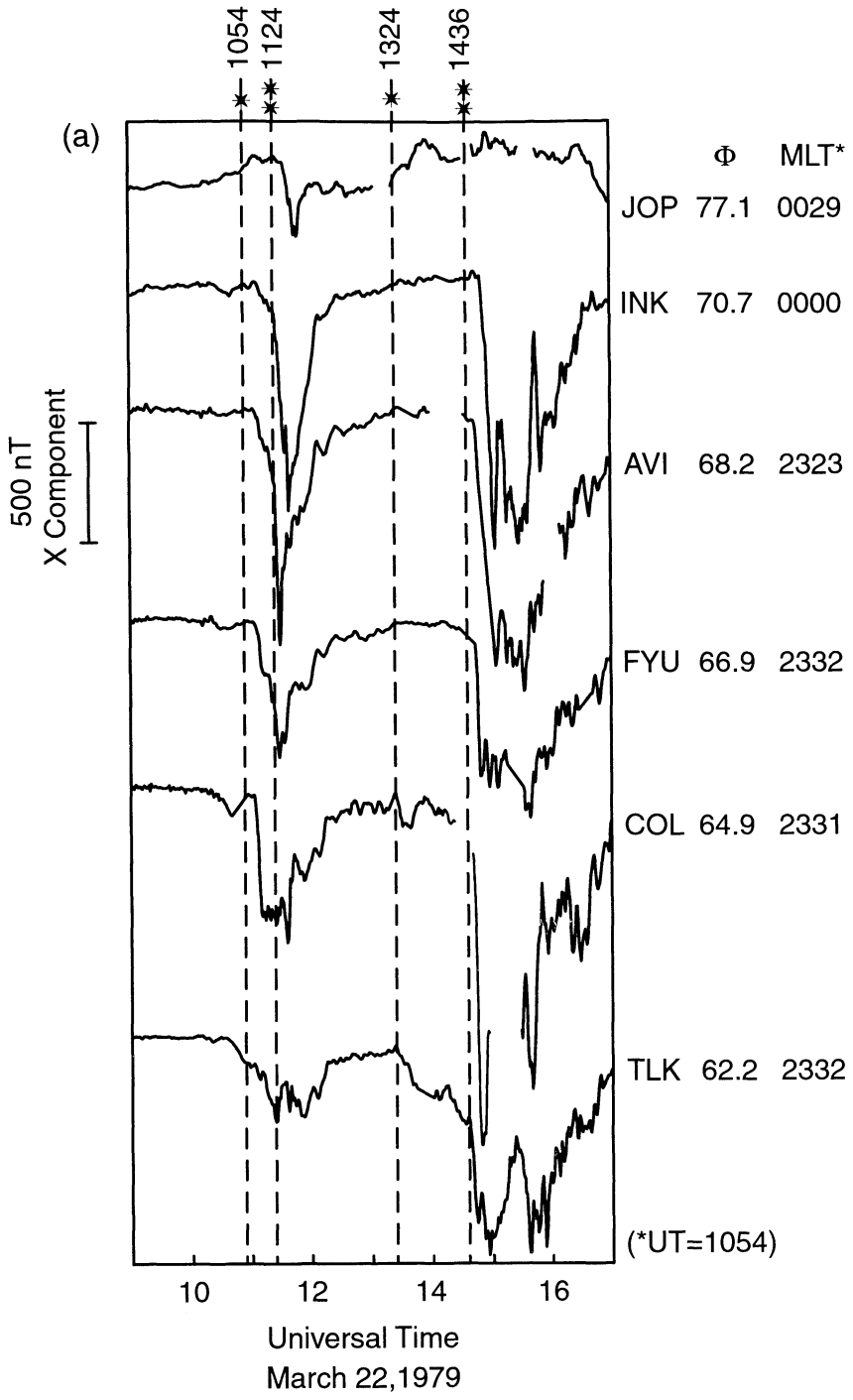

Figure 3. (a) Magnetograms of the ground-based magnetometers of the Alaskan chain, which recorded the substorm onsets of CDAW6 substorms on March 22, 1979. One and two asterisks, mark the initial and expansion onsets, respectively.

(b) The same as in Figure 3a, but for the Canadian chain.

(c) Magnetograms of the ground-based magnetometers of the Alaskan and Canadian chains, which recorded the substorm onsets of CDAW9C substorm on May 3, 1986. One and two asterisks mark the initial and full expansion onsets, respectively.

The plot of Ψ_1 for the average substorm is shown in Figure 6 together with the superposed magnetograms of two onset types, taken from Figures 4b and 4c. One can see that two types of substorm onsets correspond to the stages of growth and decrease of open flux Ψ_1, respectively. These two stages contain, respectively, the loading and unloading phases of the substorm. Of course, the loading and unloading may both be present in each of these phases but with essentially different proportions.

A sharp drop of the open magnetic flux value is the necessary signature of the classical substorm expansion onset. Hence it follows from Figure 6 that the last substorm onset, that is, that of the second type, can be called the classical expansion onset, if the

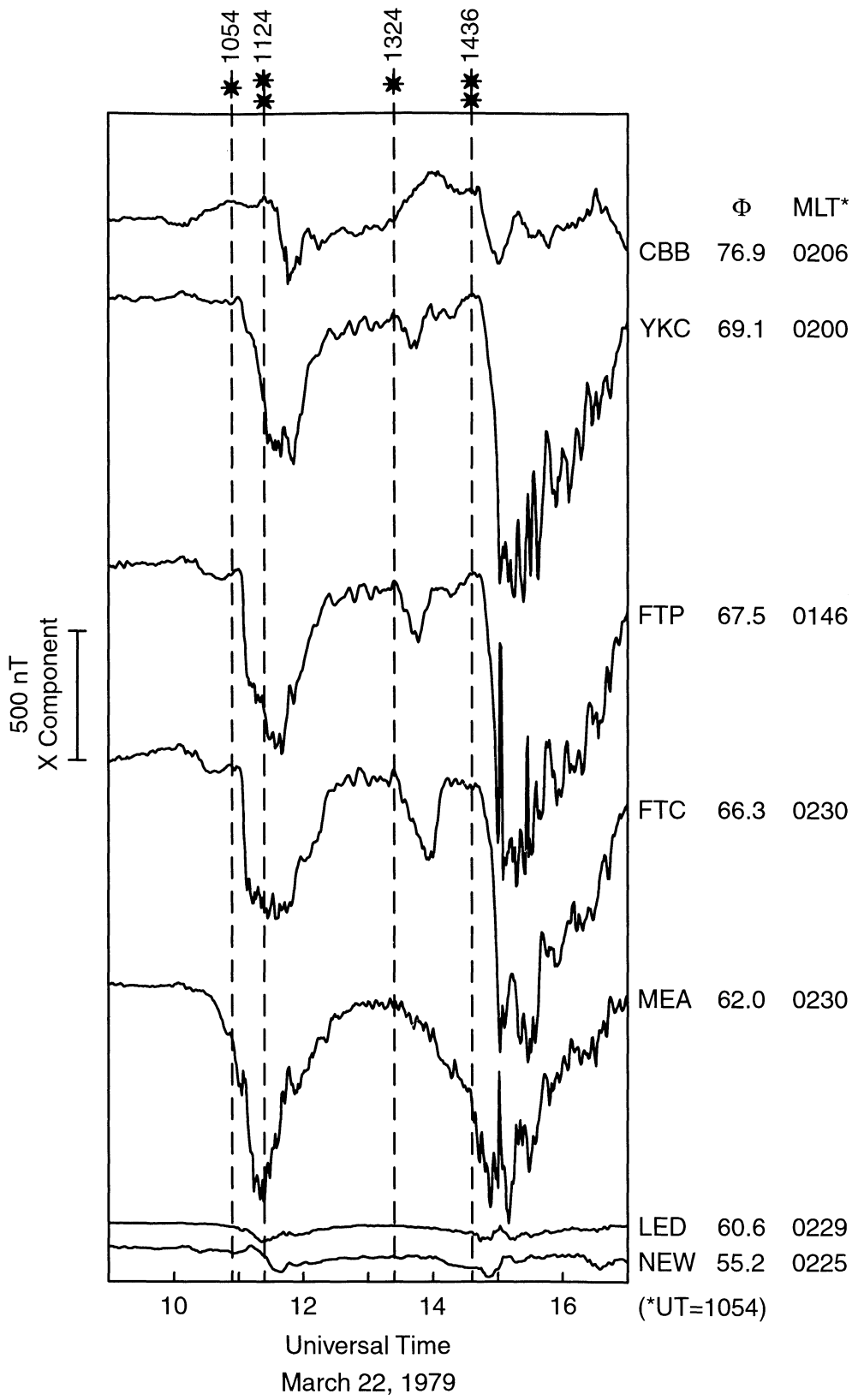

Figure 3. (continued)

other necessary and sufficient signatures are satisfied. It follows also that the onset of the first type most likely did not involve open flux reconnection and will be called initial onset herein.

The continuity equation for the variable open magnetic flux Ψ_1 is [*Russell*, 1979],

$$M\text{-}R = 2(d\Psi_1/dt), \quad (1)$$

where the factor 2 is for the two hemispheres, M is the magnetic merging rate at the dayside neutral point, and R is the reconnection rate at the nightside neutral point.

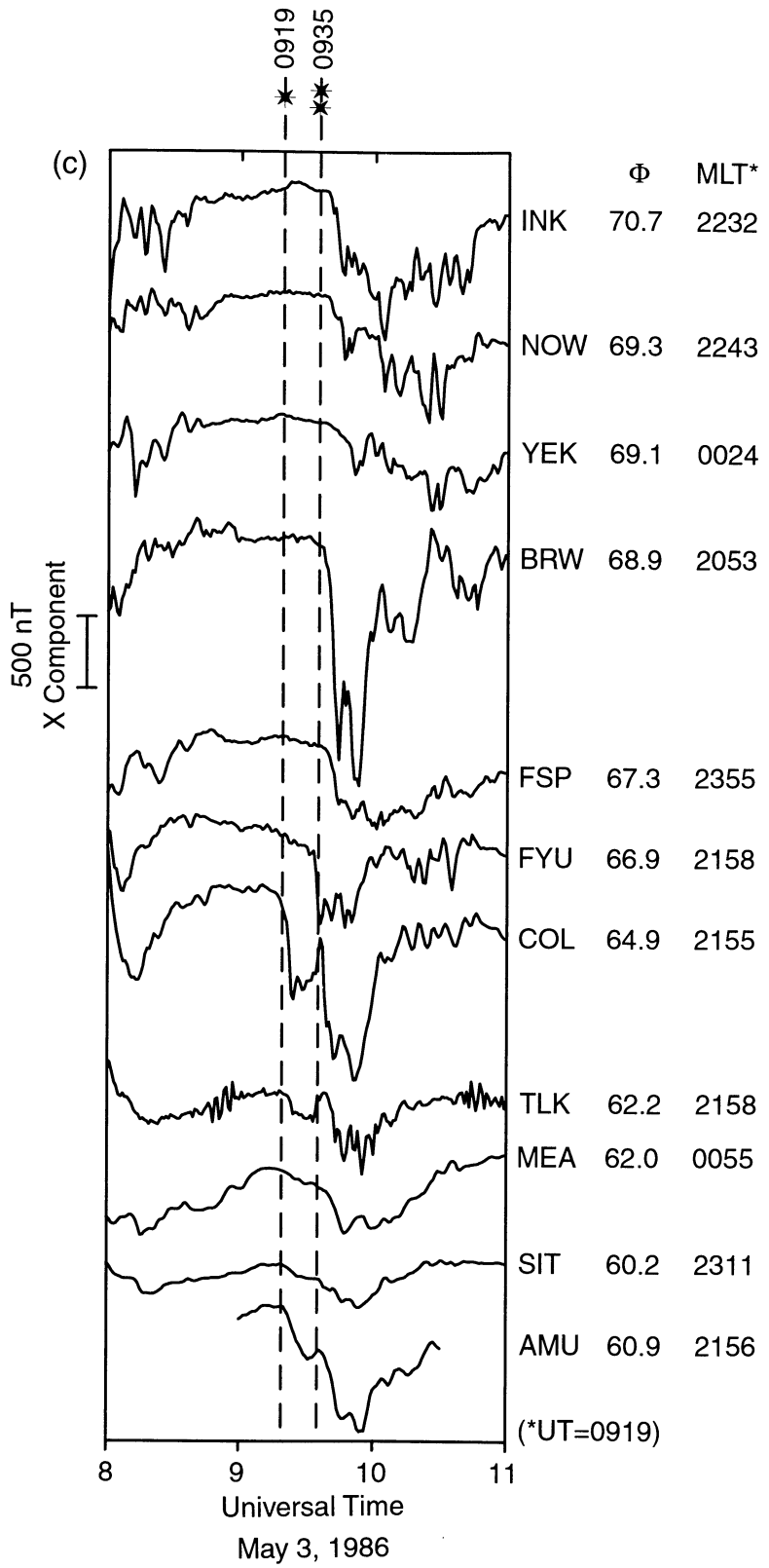

Figure 3. (continued)

The equation for M from *Kan and Lee* [1979] provides a rough estimate of M:

$$M = \sqrt{10^{-7}}\,\varepsilon V, \qquad (2)$$

where ε is the well-known Perreault-Akasofu index. As V has an almost constant value on the scale of the substorm (see Figure 2), the plot of the M variation is similar to that of ε; see Figure 9.

The next MIT2 parameter, to be used here, is the Poynting flux into the magnetosphere from solar wind ε which is approximately calculated using Ψ_1 and a formula from [*Mishin et al.*, 2000]

$$\varepsilon' = \frac{\psi_1^2 V}{\mu_0 S_T} \qquad (3)$$

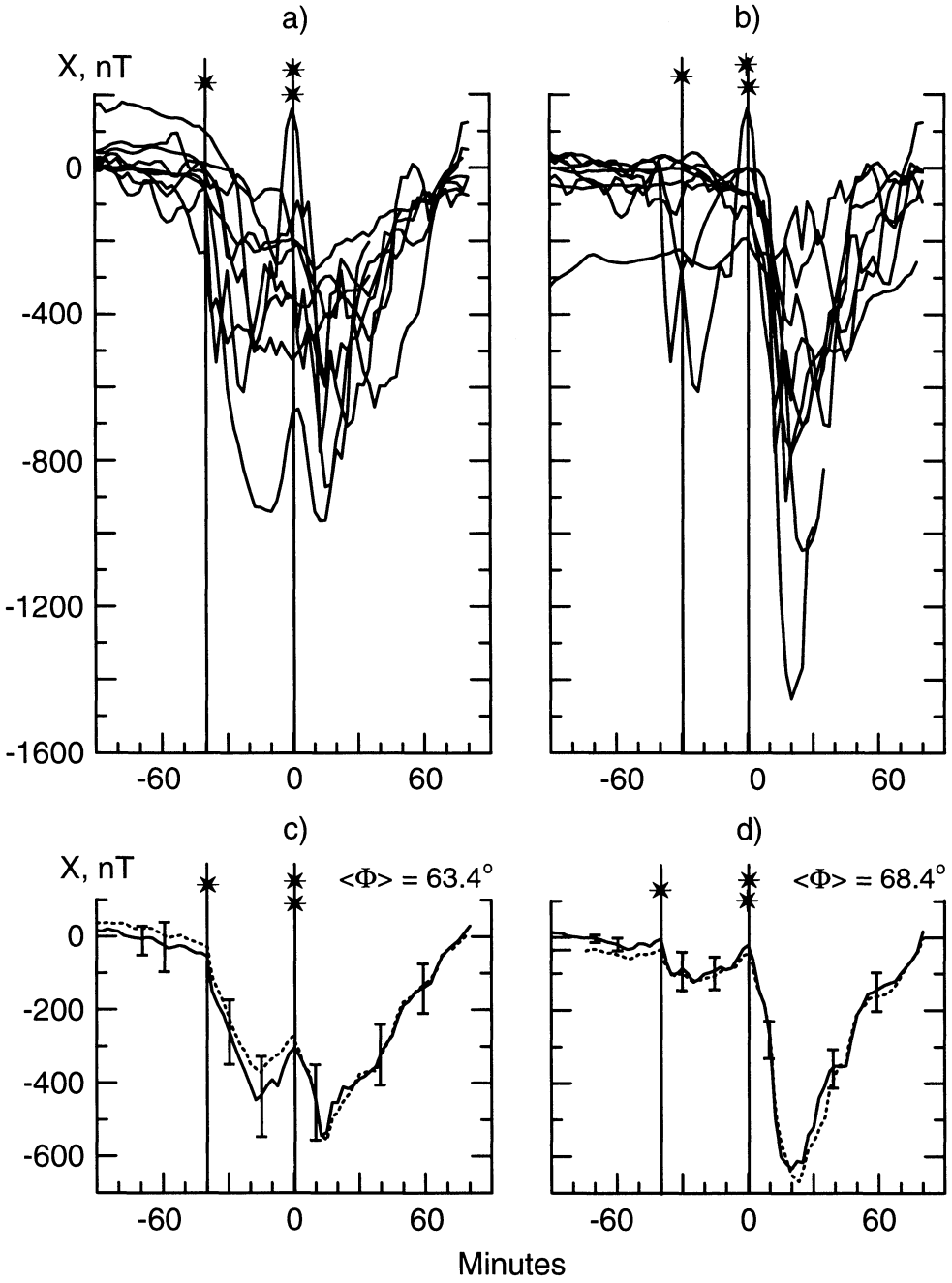

Figure 4. Normalized magnetograms of those magnetometers, which recorded (a) the strongest initial and (b) full expansion onsets Each plot corresponds to (c and d) one of the substorms: Superposed tracks obtained by data of Figures 4a and 4b, respectively. Two types of the onsets are clearly seen, and in different latitudes, <Φ>~63° and 68°, respectively. Solid and dashed lines correspond to superposition of events 7 and 9, respectively (see text).

where $S_T=\pi(R_T)^2$ with R_T, the tail's radius, taken to be equal to 22.5 R_E. The plot of ε' for the average substorm will be presented and discussed in the next section.

The Poynting flux (3) is used here jointly with a total substorm power Q_T, which is calculated as

$$Q_T = Q_{DR} + 2Q_i + 2\,Q_A \tag{4}$$

$$Q_{DR} = 4\times10^{13}(d\overline{D}_{st}/dt + \overline{D}_{st}/\tau) \tag{5}$$

where Q_i and Q_A are, respectively, the power of Joule heating and particle precipitation in the auroral ionosphere, and τ is the *DR*-current decay time that was estimated in this work according to *Clua de Gonzalez et al.* [1994]. The values of Q_i and Q_A were calculated using the empirical formulas of *Ahn et al.* [1983].

However, values of τ are known with significant uncertainty. Therefore, to be more convincing, we use yet another method, which allows us to calculate the total substorm power Q_T by making use of ε', *Dst*, and *AE* indices, without using τ. This is a slightly changed version of the method [*Mishin et al.*, 1998], which is based on the simplifying assumption that the first two phases of the substorm sequence, that is, the growth phase and first active phase, are both pure loading phases, with unloading neglected. This is only an approximation, of course. However,

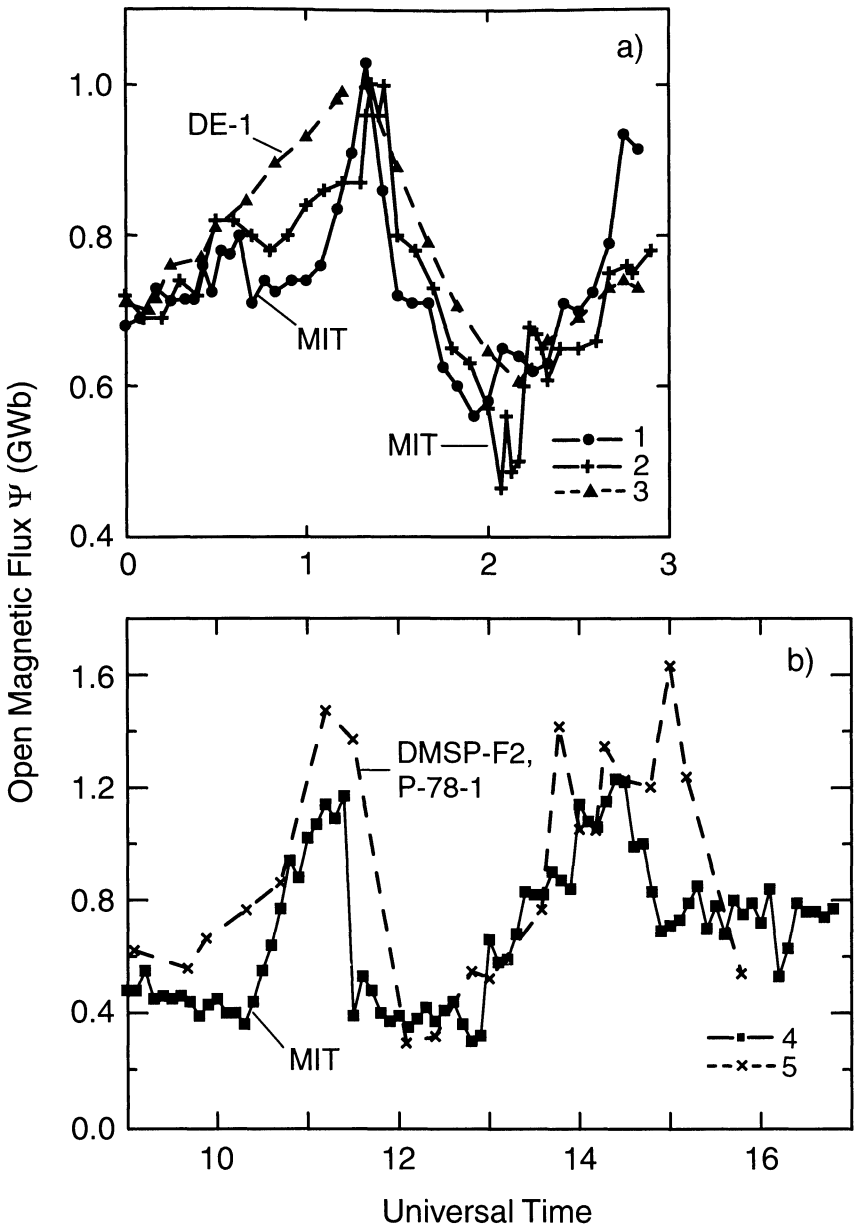

Figure 5. Variations of the magnetic flux through the polar cap in the course of the substorm of (a) May 3, 1986, 0000-0300 UT, and of (b) March 22, 1979, 0900-1700 UT. Numerals refer to 1, MIT2 data, spectrum of spherical harmonics, n=26 and m=4; 2, MIT2 data, spectrum of spherical harmonics; n=40 and m=4; 3, DE 1 data [*Baker et al.*, 1994], 4. MIT2 data, spectrum of spherical harmonics; n=26 and m=4; 5, DMSP-F2 data [*Holzer et al.*, 1986].

this method gives values of Q' close to the values of Q_T obtained using the classical approach with (4) and (5); see Figure 9. Therefore we will change the values of Q_T for Q^T and vice versa in some equations of the next Section and Table 2, which is the second goal of using Q^T in this paper. The equations for calculating Q^T are as follows.

Since our data show that $M>R$ during the loading phase, let us assume that R is negligible during this phase. Let then t_1, t_2, t_3, and t_4 be, respectively, the start times of the four successive substorm phases, and t_5 be the end of the recovery phase. Then, for the loading stage including the border of this stage, $t=t_3$, the equation

$$Q^T(t) = k\varepsilon'(t) \tag{6}$$

holds, with k <1 being the unknown coefficient, and the energy, stored during whole substorm sequence, is

$$W = (1-k)<\varepsilon'>(t_5 - t_1). \tag{7}$$

Angle brackets indicate average over the interval (t_1, t_5) herein. For two unloading phases we assume a linear dependence of Q^T from both the AE index and the average power $W/(t_5 - t_3)$. The assumed dependence has the form

$$Q^T(t) = k\varepsilon'(t) + [W/(t_5 - t_1)]AE(t)/<AE> \tag{8}$$

for $t_3 < t < t_5$. The same equation is assumed to hold at the border, $t=t_3$, but without the first term on the right. Equations (6) to (8), with the above mentioned boundary condition, comprise the total

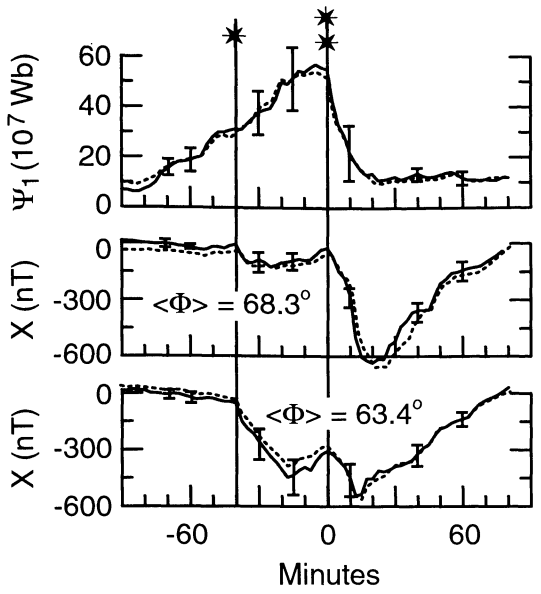

Figure 6. Plot of Ψ_1 variation and superposed normalized X magnetograms for two types of substorm onsets. Solid and dashed lines correspond to superposition of 7 and 9 events, respectively.

system with given ε' (t) and the values of t_n, n=1 to 5. Thus the function Q^T (t) can be calculated for both, loading and unloading, substorm phases. The values of the coefficient k were found to change from event to event between 0.3 and 0.7, being k=0.47 for the average substorm.

The values of ε', Q_T, and Q^T are used to obtain the differences $P=(\varepsilon'-Q_T)$ and $P'=(\varepsilon'-Q^T)$. The sign of P (or P') indicates which regime, loading or unloading, predominates at the time interval under consideration. If $P>0$ and $P'>0$, the loading regime prevails, and hence this substorm phase is largely a directly driven one (although the substorm bursts during this phase are likely caused by intramagnetospheric instabilities). For $P<0$ and $P'<0$, quite the reverse is observed: an intramagnetospheric energy source and an unloading regime are both dominant. Thus the inequalities $P>0$ ($P'>0$) and $P<0$ ($P'<0$) are the signatures of two loading and two unloading substorm phases, respectively, as well as of the initial and expansion onsets, respectively.

The values of P and P' are plotted in Figure 7 together with two superposed magnetograms from Figures 4b and 4c. One can see that for the initial onset and the whole interval $t<0$ the inequalities $P>0$ and $P'>0$ both hold, while for the last onset and the whole interval $t<0$ the inequalities $P<0$ and $P'<0$ hold (within some minutes). These results also support the above conclusion that two different physical processes correspond to the initial and last onset of the average substorm sequence shown here.

Knowing the equivalent current system, the parameter t_w can be found, that is, the magnetic local time of the western end of the westward electrojet, which coincides with the Harang discontinuity center. The parameter t_w serves as an indicator of the type of equivalent current system: the type is *DP* 2 when $t_w \approx 23$ MLT, and t_w close to 18 MLT corresponds to the *DP* 1 type. (For a discussion of the *DP* 1 (substorm) and *DP* 2 (convection) current systems, see *Nishida* [1971] and *Pudovkin* [1974]. The *DP* 2 to *DP* 1 transition is the result of the cross-tail current disruption, which produces a current wedge and thereby strengthens the ionospheric westward electrojet [e.g., *McPherron et al.*, 1973, and references therein]. The overall current system is altered: the morning current vortex (containing the westward electrojet) is enhanced, and the evening current vortex is partially suppressed. The system becomes a quasi-one vortex, which is denoted by the symbol *DP* 1.

For an example of the *DP* 2 to *DP* 1 transition, see Figure 8. Here "clean" *DP* 2 and "clean" *DP* 1 are observed, respectively, at 0105 UT and 0140 UT on May 3, 1986. It is evident that the *DP* 2 to *DP* 1 transition is characterized by a change of t_w from ~23 MLT to ~16 MLT. Such variations of t_w are typical of substorm onsets, and, as it follows from the foregoing discussion, characterize current wedge dynamics.

It is evident in Figure 8 that the *DP* 2 to *DP* 1 transition is the property of both types of onsets, be it the initial or the last onset. However, this transition, that is, the decrease of the t_w value, appears only weakly during the initial onset of the average substorm sequence. The range and the rate of t_w decrease as both grow sharply during the last onset. Thus the plot of t_w values gives further support to the fact that the last onset, as distinct from the initial onset, is a more global one.

To summarize, all above described plots are collected in Figure 9 with the addition of some other plots obtained by the same method of superposed epochs. Added are the plots of the Perreault-Akasofu index ε, dayside merging velocity M (calculated by (2)), and *AE* and *Dst* indices. It is known that the commencement of an expansion onset is observed often, though not always, to be triggered by a decrease of the dawn-dusk interplanetary electric field [*Russell*, 1976; *Caan et al.*, 1977]; therefore it is not surprising that the start of the ε drop is observed in our super-

Table 2. Principal Characteristics of the Two Types of Onsets of the Average Substorm.

Initial Onset	Expansion Onset
Observed in ground magnetograms near Φ~63° that correspond to $\|x\|<10$ R_E in the nightside neutral sheet.	Observed between 63° ≤ Φ≤ 70° a range that includes $\|x\|>30$ R_E.
Commencement usually spontaneous (while sometimes triggered by a decrease of dayside reconnection rate).	Commencement usually triggered by a decrease of dayside reconnection rate (while sometimes spontaneously).
Is observed when the open flux Ψ_1 grows.	Is observed when the open flux begins to drop.
Tail stretches, although a local dipolarization is observed simultaneously in the inner region.	Tail collapses.
$P_2=\varepsilon'_2-Q_T>0$.	$P_3=\varepsilon'_3-Q_1<0$.
Current wedge has a longitudinal size of ~3 hours.	Current wedge has a longitudinal size of ~6 hours.
The threshold values are: $\Psi_1\approx 0.28$ GWb, and $W\approx 1\times 10^{15}$ Joule in Figure 9.	The threshold values are: $\Psi_1\approx 0.5$ GWb, and $W\approx 2.7\times 10^{15}$ Joule in Figure 9.
Average input power $<\varepsilon'_2>\approx 1500$ GW.	$<\varepsilon'_3>\approx 300$ GW.
Average power $Q_2\approx 500$ GW.	$Q_3\approx 1000$ GW.
Tail reconnection rate $R_2\approx 230$ kV.	$R_3\approx 330$ kV.
Rate of plasma inflow into reconnection region $V_2^{in}\approx$ (3 to 12) km/s	$V_3^{in}\approx$ (23 to 31) km/s
Relative reconnection rate is M_{a2}=0.002-0.012.	M_{a3}=0.01-0.015.

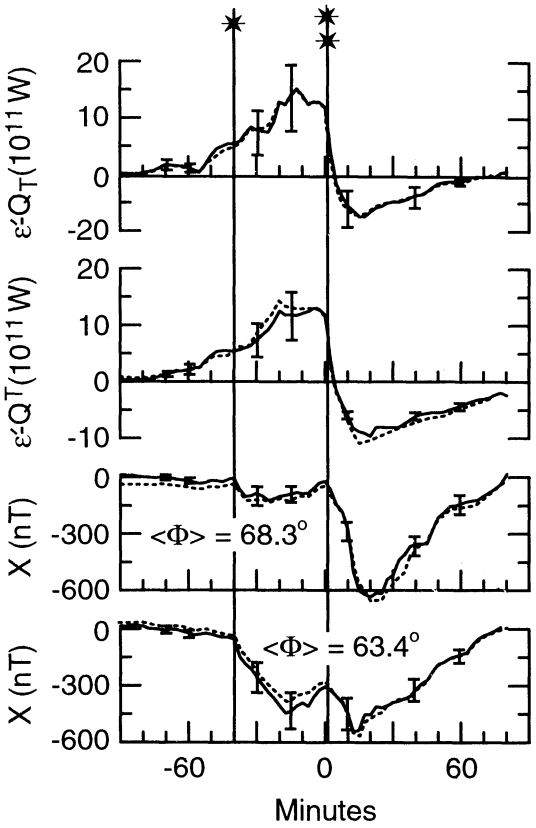

Figure 7. Plots of differences between input and consumed energy fluxes, $P_1=\varepsilon'-Q_T$ and $P_2=\varepsilon'-Q^T$, and superposed normalized X magnetograms for two types of substorm onsets. Solid and dashed lines correspond to superposition of 7 and 9 events, respectively.

posed traces as the trigger of the last substorm onset and an abrupt increase of the *AE* indices. In contrast, in the average substorm the initial onset and the subsequent first active phase occur spontaneously, without any correlation with variations of ε. Using data on magnetic field dipolarization at synchronous orbits, *Pudovkin et al.* [1990a, 1990b] also identified two types of substorm onsets, the first, spontaneous, and the second, stronger, and triggered by a northward turning of the IMF.

Such are the statistical results. In individual substorms, we sometimes observed the opposite situation, with initial onsets triggered by a drop of the ε value and spontaneous expansion onsets.

The initial onset marks the start of the first active phase in our average substorm sequence. Note again that in many known individual events, the first active phase is known to contain multiple onsets, all of which refer to the first type. Besides, according to *Rostoker* [1998], the pseudobreakups are observed during the phase of Ψ growth, so that they have the principal signature of the initial onset. It is known that pseudobreakups are accompanied by an intensification of auroral arcs, an enhancement of the westward auroral electrojet, Pi2 pulsations, and almost all other signatures of expansion onset, but the disturbance in the course of an individual onset is more likely to "quiet down" before it attains the size of a full expansion onset. This phenomenon of "quenching" is a major outstanding problem.

5. Power and Reconnection Rate

MIT2 parameters are used in this section to compare the powers and reconnection rates characteristic of the two above-mentioned types of onsets. The Poynting flux from the solar wind to the geomagnetosphere ε′, and the reconnection rate at the dayside magnetopause M, are calculated by (3) and (2), respectively. The substorm power and stored energy will be calculated using (6) to (8), and taking into account that, as it was mentioned in the previous section, $Q^T \approx Q_T$. In the following, we will use the subscripts as the substorm phase numbers only. The symbols Ψ_m and Q_m will denote, respectively, Ψ_1 and Q_T in the mth phase (e.g., Ψ_3 is the value of Ψ_1 in the second active phase). With these notations, and in view of the above mentioned formulas, the mean powers of two active phases or, in other words, of two successive types of substorm onsets, are respectively

$$<Q_2> = \kappa<\varepsilon'_2> \quad (9)$$

$$<Q_3> = W/\tau_3. \quad (10)$$

The mean rates of reconnection in the plasma sheet or partial cross-tail current disruption are

$$<R_3> = \Delta\Psi_3/\tau_3+<M_3> \quad (11)$$

$$<R_2> = <M_2>\sqrt{k}. \quad (12)$$

Assuming that Q_m is produced by the magnetic energy flux into the reconnection region with the area S_n and magnetic field B_n, we have the inflow rate

$$V_m^{in} = \mu_0 Q_n/B_n S_n \quad (13)$$

$$M_{am} = V_m^{in}/V_{am}, \quad (14)$$

where V_a (km^{-1}/s)=22B(nT)/$\sqrt{n}$(cm^{-3}) is the Alfven velocity and M_a is the relative rate of reconnection or cross-tail current partial disruption.

For estimating V_m^{in} and M_{am}, we assumed that B_2 and B_3 are the characteristic values of the magnetic field strength on the midnight meridian, respectively, in the plasma sheet, $|x|$=5 to 10 R_E, during the growth phase, and in the tail lobe, $|x|$=20 R_E, during the expansion phase, Kp=4. According to data from *Sergeev and Tsyganenko* [1982, Figure 12] and *Pulkkinen et al.* [1992, Figure

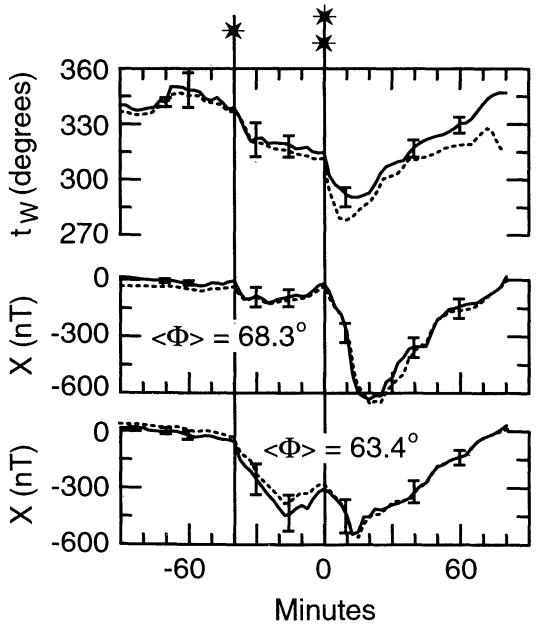

Figure 8. Plot of the variation of the parameter t_w and superposed normalized X component magnetograms of two types of substorm onsets. Solid and dashed lines correspond to superposition of 7 and 9 events, respectively.

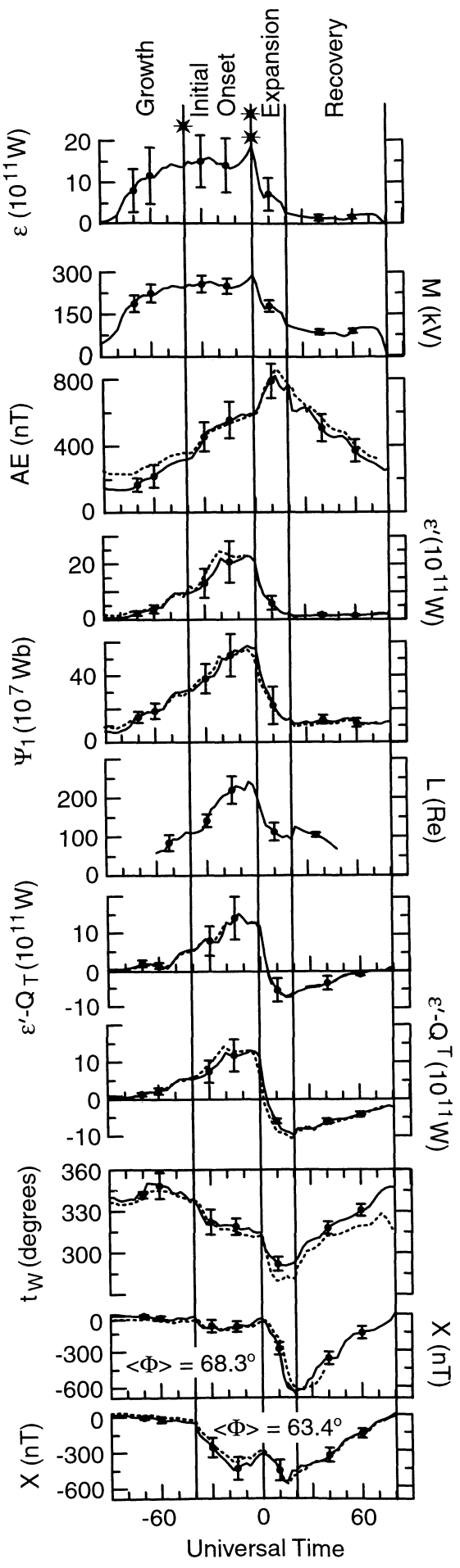

6], the values of B_2 are 40 and 80 nT, respectively. For B_3 the value 25 nT was assumed. The values of S_2 and S_3 are, by definition, the disturbed areas of the current sheet, characteristic for the initial onset and expansion onset, respectively. According to *Mishin et al.* [1998], the interval 0112 to 0116 UT on May 3, 1986 can be used as a representative of the initial onset, m=2, for which the data were available by *Pulkkinen et al.* [1995, Plate 2]. Thus the value of S_2=3.2 × 10^{16} m^2 was determined, and the value of S_3=2S_2 has been supposed. Using data of *Borovsky et al.* [1998, Figure 1] and of *Baumjohann and Treumann* [1996, Figure 4.2], the value of n_2=0.7 cm^{-3} was taken as representative of a plasma sheet density at $|x|$=10 R_E, and n_3=0.2/30=0.07 cm^{-3} as the representative of plasma density in the tail lobes. With Q_2=5×10^{12} W, Q_3=1.0×10^{12} W (from Figure 9), the calculated values are given in Table 2.

6. Discussion

The substorm behavior we describe in this paper appears to occur frequently and be an important feature of the substorm process. We have used well-documented events examined in community-wide studies such as the March 22, 1979, CDAW6 event [*McPherron and Manka*, 1985], the May 3, 1986, CDAW9C event [*Baker et al.*, 1993] and the July 24, 1986 event [*Lui et al.*, 1995]. We have calculated standard error bars and find that the variations are significant as judged from the probable errors of the means. While many of the onsets occurred in the Canadian and Alaskan sectors, which lie to the east of a region sparsely covered with magnetometers, the fact that we need these stations only for timing the onsets and do not need to follow the full denouement of the expansion phase mitigates against the effects of this gap in coverage. Moreover, we use the MIT2 inversion technique to determine the global behavior of the magnetospheric system from all available data. These magnetospheric parameters are well correlated with our onsets as illustrated, for example, in Figures 6 and 8 where t_w correlates with the initial onset and Ψ_1 with the main expansion onset. Thus it is reasonable to examine the implication of these two onsets for our understanding of the substorm process.

6.1. On Two Different Types of Substorm Onsets

The data of Figure 9 and Table 2 suggest that at times a substorm sequence occurs with the successive development of two different types of substorm onsets. The first type develops concurrently with a growth of open flux Ψ_1. The inequality P_2=ε'_2-Q_T >0 holds for this type of onset, indicating that the initial onsets are likely created without open tail reconnection. The opposite situation occurs during the second type with P_3=ε'_3-Q_T<0. These substorm onsets are associated with a sharp, profound drop of the open flux Ψ_1, which means the global tail collapses with the severance of the large-scale plasmoid. Data for the average substorm sequence also demonstrate that the instabilities responsible for each of these onsets differs by the values of Ψ, stored energy W, and cross-tail current density and intensity during onset.

The short-time substorm intensifications lasting ~10 min have various names in the literature: trigger bays, substorm onsets, microsubstorms, multiple onsets, pseudobreakups for the first group

Figure 9. Summary of the average substorm sequence from Figures 3 to 8. Added are plots of Poynting fluxes ε and ε′, and dayside reconnection rate M. Solid and dashed lines correspond to superposition of 7 and 9 events, respectively.

of intensifications, and expansion onset or full breakup for the second group. Our data suggest that the first group of intensifications are typically observed before the last global expansion onset, that is, in the loading stage, when Ψ and stored energy W are growing, the inequality $P>0$ holds, and the *DP* 2 type is observed, rather than *DP* 1. Thus the term initial onset can supposedly be considered as a generalization of the whole first group of terms (though some special breakups may be separated, which are observed in higher latitudes than the initial onsets discussed here). We emphasize that the two-stage nature of the onset of substorms was first recognized many years ago [*Rostoker*, 1968] and attributed to reconnection first on the magnetopause and then later in the tail. Our contribution is to make the argument that both onset points are in the tail and correspond to closed flux and open flux reconnection. Thus the initial onset may be considered, not as a trigger, but as a precursor to the classical expansion onset.

If the above postulate is true, one of the known outstanding questions, which was earlier formulated for the pair of pseudo and full breakups, may now be reformulated as follows: Why are the initial onsets quenched without the transition to the regime of open flux reconnection? Such a question has a special meaning if it is assumed that the initial and classical expansion onsets have not only a similar morphology but also similar physics. Such a view seems to be supported by observations [e.g., *Nakamura et al.*, 1994; *Aikio et al.*, 1999]. One possible answer is that the two onsets are caused by different instabilities with different thresholds. Another possible answer has been given by *Russell* [2000], who attributes the two onsets to reconnection in the presence and absence of active reconnection at the distant neutral point and who discusses how the direction of the IMF can affect the interplay between the two neutral points.

6.2. Substorm as a Global Instability

Mishin et al. [1997] assumed that under certain assumptions (3) can be rewritten as

$$\varepsilon' = M^2 L^2 / \mu_0 S_T V. \qquad (15)$$

Hence it follows that when M is constant, that is, under steady state external conditions, the energy flux to the magnetosphere ε' is controlled by the tail length L. On the other hand, it is known that the tail length is determined by the strength of the cross-tail current, which is proportional to stored energy. Hence L grows with increasing ε'. This direct dependence, $L \sim \varepsilon'$, together with (15), assumes an exponential growth with time of both parameters, L and ε', even if M is a nonzero constant. The generator of ε' operates in a regime of self-excitation. Indeed, it is apparent from Figure 9 that the condition M is constant is roughly satisfied over the interval $0>t>-60$ min. The data of *Mishin et al.* [1998, Figure 1] allow us to assume that L increases in this interval by a factor of about 2.5. Then ε' increases ~6 times. Such a growth of ε' when M is constant implies a strong increase of effectiveness of the primary magnetospheric power generator.

Thus, in the scenario considered, the substorm loading phase includes the development of global tail stretching, in the course of which the tail length increase several times. The *DP* 2 to *DP* 1 transition and development of the current wedge commence, and the effectiveness of the primary magnetospheric power generator increases by several times. Initial onset and associated closed flux reconnection do not stop the tail stretching. The second onset may represent a global instability that leads to a change of the global tail stretching process for the tail collapse and a large-scale rearrangement of the magnetic field and currents. The *DP* 2 to *DP* 1 transition and the development of the current wedge are then both accelerated and completed. For a discussion of how these two onsets may be related to changing conditions in the solar wind, see *Russell* [2000].

6.3. Substorms and Solar Flares

The scenario considered above contains some basic elements of two alternative substorm models and, additionally, a nonlinear global process named the tail stretching instability. Note that a similar scenario was found to be typical of big solar flares. In this scenario, two types of flare onsets exist called loop-top flares and above-loop-top flares [*Masuda et al.*, 1994]. These two types compose two active phases, which develop successively in the magnetosphere of the flare-producing region, after the growth phase, during which the magnetosphere opens and free energy, sufficient for the flare, is stored in the magnetotail. The first active phase develops in the near tail and the second phase in the middle tail of the flare-producing magnetosphere, and they are created by processes, respectively, without and with open tail reconnection [*Shibata*, 1998; *Mishin and Falthammar*, 1998, and references therein].

7. Conclusions

Substorms frequently have two onsets. The first onset is small and has been referred to as a trigger bay or a pseudobreakup among other terms. The first onset occurs at lower latitudes than the second onset and does not disrupt the continued buildup of tail magnetic flux. The second onset occurs at higher latitudes and clearly involves the reconnection of open magnetic tail flux. It is this onset that is triggered by the interplanetary magnetic field turning northward and it is the main expansion onset. These two types of substorm onsets are distinct physical events. One of them can be interpreted within the framework of the classical NENL model but the other requires a new approach and some modification of this model.

Acknowledgments. V.M.M., A.B., and T.S. are indebted to V.D. Urbanovich and P.A. Sedykh from ISTP, Irkutsk, B. Hultqvist and K.-G. Falthammar from the Swedish Academy of Sciences, W. Campbell and H. Kroehl from WDCA, Boulder, A. Richmond and B. Emery from HAO, Boulder, G. Siscoe from the University of Boston, D.N. Baker from the University of Colorado, D. Sibeck and A.T.Y. Lui from Johns Hopkins University, and P. Reiff from Rice University for financial support and helpful discussions. This work was done with support from the Russian Foundation for Basic Research (RFBR), grants Nos. 96-05-64348, 98-05-65406, 98-05-04133, and 99-05-68234. Work at UCLA was supported by the National Science Foundation under grant ATM98-03431.

Michel Blanc thanks the two referees for their assistance in evaluating this paper.

References

Ahn, B.-H., R.M. Robinson, Y. Kamide, and S.-I. Akasofu, Electric conductivities, electric fields and auroral particle energy injection rate in auroral ionosphere and their empirical relation to the horizontal magnetic disturbances, *Planet. Space Sci., 31*, 641-653, 1983.

Aikio, A.T., V.A. Sergeev, M.A. Shuktina, L.I. Vagina, V. Angelopoulos, and G.D Reeves, Characteristics of pseudobreakups and substorms observed in the ionosphere, at the geosynchronous orbit, and in the tail, *J. Geophys. Res., 104*, 12,263-12,287, 1999.

Baker, D.N., T.I. Pulkkinen, R.L. McPherron, J.D. Craven, L.A. Frank, R.D. Elphinstone, J.S. Murphree, J.F. Fennell, R.E. Lopez, and T. Nagai, CDAW9 analysis of magnetospheric events on May 3, 1986: Event C, *J. Geophys. Res., 98*, 3815-3834, 1993.

Baker, D.N., T.I. Pulkkinen, R.L. McPherron, and C.R. Clauer, Multi-

spacecraft study of a substorm growth and expansion phase features using a time-evolving field model, in *Solar System Plasmas in Space and Time, Geophys. Monogr. Ser., vol. 84*, edited by J.L. Burch and J.H. Waite Jr., pp. 101-110, AGU, Washington, D. C., 1994.

Baker, D.N., T.I. Pulkkinen, V. Angelopoulos, W. Baumjohann, and R.L. McPherron, Neutral line model of substorms: Past results and present view, *J. Geophys. Res., 101*, 12,975-13,010, 1996.

Baker, D.N., T.I. Pulkkinen, J. Büchner, and A.J. Klimas, Substorms: A global instability of the magnetosphere-ionosphere system, *J. Geophys. Res., 104*, 14,601-14,611, 1999.

Baumjohann, W. and R.A. Treumann, *Basic Space Plasma Physics*, 330 pp, Imperial Coll. Press, London, 1996.

Borovsky, J.E., M.F. Thomsen, and R.C. Elphic, The driving of the plasma sheet by the solar wind, *J. Geophys. Res., 103*, 17,617-17,639, 1998.

Caan, M.N., R.L. McPherron, and C.T. Russell, Characteristics of the association between the interplanetary magnetic field and substorm, *J. Geophys. Res., 82*, 4837-4842, 1977.

Clua de Gonzalez, A.L., W.D. Gonzalez, T.R. Detman, and J.A. Joselyn, Evolution of the magnetospheric storm-ring current with a constant time delay, in *Proceedings 1994 International Conference on Plasma Physics, vol 2*, edited by P.H. Sakanaka, E. Del Bosco, and M.V. Alves, pp. 226-229, Inst. Nac. De Pesqui. Espaciais, Sao Jose des Campos, Brazil, 1994.

Erickson, G.M., W.J. Burke, M. Heinemann, J.S. Samson, and N. Maynard, Towards a complete conceptual model of substorm onsets and expansions, in *Proceedings of ICS-3, Eur. Space Agency Spec. Publ., ESA SP 389*, 423, 1996.

Fox, N.J., et al., A multipoint study of a substorm occurring on 7 December 1992 and its theoretical implications, *Ann. Geophys., 17*, 1369-1384, 1999.

Holzer, R.E., R.L. McPherron, and D.A. Hardy, A quantitative empirical model of the magnetospheric flux transfer process, *J. Geophys. Res., 91*, 3287-3293, 1986.

Hones, E.W. Jr., Transient phenomena in the magnetotail and their relation to substorms, *Space Sci. Rev., 23*, 393-410, 1979.

Iijima, T., and T.A. Potemra, The amplitude distribution of field-aligned currents at northern high latitudes observed by Triad, *J. Geophys. Res., 81*, 2165-2174, 1976.

Kamide, Y., A.D. Richmond, and S. Matsushita, Estimation of ionospheric electric fields, ionospheric currents, and field-aligned currents from ground magnetic records, *J. Geophys. Res., 86*, 801-813, 1981.

Kan, J.R., A globally integrated substorm model: Tail reconnection and magnetosphere-ionosphere coupling, *Geophys. Res. Lett., 103*, 11,787-11,795, 1998.

Kan, J.R., and L.C. Lee, Energy coupling function and solar wind-magnetosphere dynamo, *Geophys. Res Lett., 6*, 577-580, 1979.

Liou, K., C.-I. Meng, A.T.Y. Lui, P.T. Newell, M. Brittnacher, G. Parks, G.D. Reeves, R.R. Anderson, and K. Kumoto, On relative timing in substorm onset signatures, *J. Geophys. Res., 104*, 22,807-22,817, 1999.

Lui, A.T.Y., Current disruption in the Earth's magnetosphere: Observations and models, *J. Geophys. Res., 101*, 13,067-13,088, 1996.

Lui, A.T.Y., R.D. Elphinstone, J.S. Murphree, M.G. Henderson, H.B. Vo, L.L. Cogger, H. Lühr, S. Ohtani, P.T. Newell, and G.D. Reeves, Special features of a substorm during high solar wind dynamical pressure, *J. Geophys. Res., 100*, 19,095-19,107, 1995.

Lui, A.T.Y., et al., Multipoint study of a substorm on February 9, 1995, *J. Geophys. Res., 103*, 17,333-17,343, 1998.

Masuda, S., T. Kosugi, H. Hara, S. Tsuneta, and Y.A. Ogawara, A loop-top hard X-ray source in a compact solar flare as evidence for magnetic reconnection, *Nature, 371*, 495-497, 1994.

Maynard, N.C., W.J. Burke, G.M. Erickson, E.M. Basinska, and A.G. Yahnin, Magnetosphere-ionosphere coupling during substorms onset, in *Proceedings of ICS-3, Eur. Space Agency Spec. Publ., ESA SP 389*, 301, 1996.

Maynard, N.C., et al., Geotail measurements compared with the motions of high-latitude auroral boundaries during two substorms, *J. Geophys. Res., 102*, 9553-9572, 1997.

McPherron, R.L., and R.H. Manka, Dynamics of 1054 UT March 22, 1979, substorm event: CDAW 6, *J. Geophys. Res., 90*, 1175-1190, 1985.

McPherron, R.L., C.T. Russell, and M.P. Aubry, Satellite studies of magnetospheric substorms on August 15, 1968, IX, Phenomenological model for substorms, *J. Geophys. Res., 78*, 3131-3149, 1973.

Mishin, V.M., The magnetogram inversion technique: Applications to the problem of magnetospheric substorms, *Space Sci. Rev., 57*, 237-337, 1991.

Mishin, V.M., and C.-G. Falthammar, Pseudo and true substorm onsets within framework of the analogy, magnetospheric substorms-solar flares, , *Eur. Space Agency Spec. Publ., ESA SP (ICS-4)*, p. 731, 1998.

Mishin V.M., A.D. Bazarzhapov, T.I. Saifudinova, S.B. Lunyushkin, D.Sh. Shirapov, J. Woch, L. Eliasson, H. Opgenoorth, and J.S. Murphree, Different method to determine the polar cap area, *J. Geomagn. Geoelectr., 44*, 1207-1214, 1992.

Mishin V.M., et al., A study of the CDAW9C substorm, May 3, 1986, using magnetogram inversion technique 2, and a substorm scenario with two active phases, *J. Geophys. Res., 102*, 19,845-19,859, 1997.

Mishin, V.M., V.D. Urbanovich, G.B. Shpynev, T.I. Saifudinova, A.D. Bazarzhapov, and D.S. Shirapov, Substorm-Storm Relationships, Substorms-4, *Eur. Space Agency Spec. Publ., ESA SP (ICS-4)*, 801-804, 1998.

Mishin, V.M., C.T. Russell, T.I. Saifudinova, and A.D. Bazarzhapov, Study of weak substorms observed during December 8, 1990, Geospace Environment Modeling campaign: Timing of different types of substorm onsets, *J. Geophys. Res.*, 105, 23,263-23,276, 2000.

Nagai, T., M. Fujimoto, Y. Saito, S. Machida, T. Terasawa, R. Nakamura, T. Yamamoto, T. Mukai, A. Nishida, and S. Kokubun, Structure and dynamics of magnetic reconnection for substorm onsets with Geotail observations *J. Geophys. Res., 103*, 4419-4440, 1998.

Nakamura, R., D.N. Baker, T. Yamamoto, R.D. Belian, E.A. Bering III, J.R. Benbrook, and J.R. Theall, Particle and field signatures during pseudobreakup and major expansion onset, *J. Geophys. Res., 99*, 207-221, 1994.

Nishida, A., Interplanetary origin of electric fields in the magnetosphere, *Cosmic Electr., 2*, 350-374, 1971.

Pudovkin, M.I., Electric fields and currents in the ionosphere, *Space Sci. Rev., 16*, 727-770, 1974.

Pudovkin, M.I., V.S. Semenov, T.A. Kornilova., and T.V. Kozelova, The development of magnetospheric substorm: Theory and experiment, I, in *Research in Geomagnetism, Aeronomy, and Solar Physics,. Issue 89*, Nauka, Moscow, p. 5, 1990a.

Pudovkin, M.I., V.S. Semenov, T.A. Kornilova, and T.V. Kozelova, The development of magnetospheric substorm: Theory and experiment, II, in *Research in Geomagnetism, Aeronomy, and Solar Physics, Issue 89*, Nauka, Moscow, p. 28, 1990b.

Pulkkinen, T.I., D.N. Baker, R.J. Pellinen, J. Büchner, H.E.J. Koskinen, R.E. Lopez, R.L. Dyson, and R.L. Frank, Particle scattering and current sheet stability in the geomagnetic tail during substorm growth phase, *J. Geophys. Res., 97*, 19,283-19,297, 1992.

Pulkkinen, T.I., D.N. Baker, R.J. Pellinen, J.S. Murphree, and L.A. Frank, Mapping of the auroral oval and individual arcs in the high-latitude morning sector, *J. Geophys. Res., 100*, 21,987-21,994, 1995.

Pulkkinen, T.I., et al., Two substorm intensifications compared: Onset, expansion, and global consequences, *J. Geophys. Res., 103*, 15-27, 1998a.

Pulkkinen, T.I., D.N. Baker, M. Wiltberger, C. Goodrich, R.E. Lopez, and J.G. Lyon, Pseudobreakup and substorm onset: Observations and MHD simulations compared, *J. Geophys. Res. 103*, 14,847-14,854,1998b.

Rostoker, G., Macrostructure of geomagnetic bays, *J. Geophys. Res., 73*, 4217-4229, 1968.

Rostoker, G., On the place of the pseudo-breakup in a magnetospheric substorm, *Geophys. Res. Lett., 25*, 217-220, 1998.

Rothwell, P.L., L.P. Block, M.B. Silevitch, and C.-G. Falthammar, A new model for substorms onsets: The pre-breakup and triggering regimes, *Geophys. Res. Lett., 15*, 1279-1282, 1988.

Russell, C.T., Reconnexion, in *Physics of Solar Planetary Environments*, vol.2, edited by D.J. Williams, pp. 526-540, AGU, Washington, D. C., 1976.

Russell, C.T., The control of the magnetopause by the interplanetary magnetic field, in *Dynamics of the Magnetosphere*, edited by S.-I. Akasofu, pp. 3-21, D. Reidel, Norwell, Mass, 1979.

Russell, C.T., How northward turnings of the IMF can lead to substorm expansion onsets, *Geophys. Res. Lett., 27*, 3257-3259, 2000.

Russell, C.T., and R.L. McPherron, The magnetotail and substorms, *Space Sci. Rev., 15*, 205-266, 1973.

Sergeev, V.A., and N.A. Tsyganenko, *The Earth's Magnetosphere*, 171 pp., Nauka, Moscow, 1982.

Shibata K., A unified model of solar flares, *Astrophysics and Space Sci-*

ence Library, vol. 229, (Observational Plasma Astrophysics: Five Years of Yohkoh and Beyond, Tokyo, Japan, 6-8 Nov. 1996) Kluwer Academic Publishers, Dordrecht, 187-196, 1998.

Taylor, J.R., T.K. Yeoman, M. Lester, B.A. Emery, and D.J. Knipp, Variations in the polar cap area during intervals of substorm activity on 20-21 March 1990 deduced from AMIE convection patterns, *Ann. Geophys., 14,* 879-887, 1996.

Tsyganenko, N.A., A magnetospheric magnetic field model with a warped tail current sheet, *Planet. Space Sci., 37,* 5-20, 1989.

Vasyliunas, V.M., Theoretical considerations on where a substorm begins, Substorms-4, in *Proceedings of ICS-4,* p. 9, Terra Sci., Tokyo 1998.

Zelenyi L.M., et al., Substorm onsets models and observations, Substorms-4, in *Proceedings of ICS-4,* p. 327, Terra Sci., Tokyo 1998.

W. Baumjohann and R. Nakamura, Space Research Institute, Austrian Academy of Sciences, Schmiedlstr. 6, A-8042 Graz, Austria, (bj@mpe.mpg.de)

A. Bazarzhapov, V. M. Mishin, and T. Saifudinova, Institute of Solar Terrestrial Physics, Russian Academy of Science, POB 4026, Irkutsk 33, Russia (Mishin@iszf.irk.ru)

M. Kubyshkina, Institute of Physics, St. Petersburg State University, 29 Politekhnitcheskaya str., St. Petersburg, 195251, Russia

C. T. Russell, Institute of Geophysics and Planetary Physics, University of California at Los Angeles, 3845 Slichter Hall, Los Angeles, CA 90095-1567 (ctrussel@igpp.ucla.edu)

(Received February 14, 2000; revised October 13, 2000; accepted October 13, 2000.)